

Communication

Fluorescent Immunoassay with a Copper Polymer as the Signal Label for Catalytic Oxidation of *O*-Phenylenediamine

Yunxiao Feng ^{1,†}, Gang Liu ^{2,3,†}, Chunhuan Zhang ³, Jinrui Li ³, Yuanyuan Li ^{2,*} and Lin Liu ^{3,*} 

¹ College of Chemistry and Chemical Engineering, Pingdingshan University, Pingdingshan 467000, China; 2743@pdsu.edu.cn

² College of Chemistry and Chemical Engineering, Henan University of Technology, Zhengzhou 450001, China; liugang08215@163.com

³ Henan Province of Key Laboratory of New Optoelectronic Functional Materials, Anyang Normal University, Anyang 455000, China; zch2142967813@163.com (C.Z.); lijnrui7022@163.com (J.L.)

* Correspondence: yuanyuanli@haut.edu.cn (Y.L.); liulin@aynu.edu.cn (L.L.)

† These authors contributed equally to this work.

Abstract: This work suggested that Cu²⁺ ion coordinated by the peptide with a histidine (His or H) residue in the first position from the free N-terminal reveals oxidase-mimicking activity. A biotinylated polymer was prepared by modifying His residues on the side chain amino groups of lysine residues (denoted as K_H) to chelate multiple Cu²⁺ ions. The resulting biotin-poly-(K_H-Cu)₂₀ polymer with multiple catalytic sites was employed as the signal label for immunoassay. Prostate specific antigen (PSA) was determined as the model target. The captured biotin-poly-(K_H-Cu)₂₀ polymer could catalyze the oxidation of *O*-phenylenediamine (OPD) to produce fluorescent 2,3-diaminophenazine (OPDox). The signal was proportional to PSA concentration from 0.01 to 2 ng/mL, and the detection limit was found to be eight pg/mL. The high sensitivity of the method enabled the assays of PSA in real serum samples. The work should be valuable for the design of novel biosensors for clinical diagnosis.

Keywords: fluorescent immunoassay; peptide; copper; *O*-phenylenediamine; prostate specific antigen



Citation: Feng, Y.; Liu, G.; Zhang, C.; Li, J.; Li, Y.; Liu, L. Fluorescent Immunoassay with a Copper Polymer as the Signal Label for Catalytic Oxidation of *O*-Phenylenediamine. *Molecules* **2022**, *27*, 3675. <https://doi.org/10.3390/molecules27123675>

Academic Editor: Silvia Angelova

Received: 10 May 2022

Accepted: 2 June 2022

Published: 8 June 2022

Publisher's Note: MDPI stays neutral with regard to jurisdictional claims in published maps and institutional affiliations.



Copyright: © 2022 by the authors. Licensee MDPI, Basel, Switzerland. This article is an open access article distributed under the terms and conditions of the Creative Commons Attribution (CC BY) license (<https://creativecommons.org/licenses/by/4.0/>).

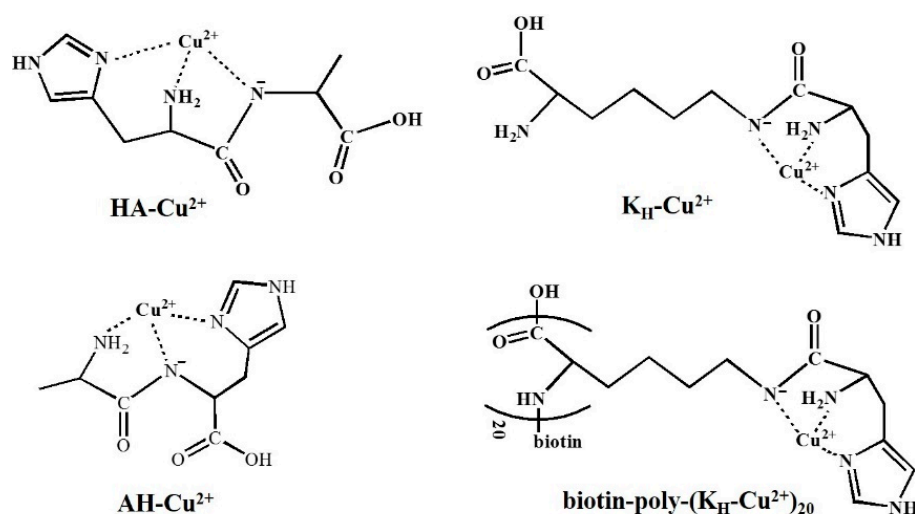
1. Introduction

Enzymes have been widely utilized as efficient signal labels in the construction of biosensors, including horseradish peroxidase (HRP), glucose oxidase (GOx) and alkaline phosphatase (ALP) [1,2]. However, the enzymatic signal amplification confronts low sensitivity because of the limited number of enzymes involved in the recognition event (generally one enzyme molecule in each event). The utilization of polymeric conjugates and nanomaterials for loading of numerous enzymes has proven to be an effective strategy to enhance the sensitivity [3,4]. However, some disadvantages, such as complicated preparation procedure, high cost, low stability and strict storage condition, seriously hamper the applications of enzyme labels [5]. Moreover, modification of enzymes on a solid surface may decrease the catalytic activity, and the large size of enzyme may cause the steric inhibition of antibody-antigen reaction. To resolve these shortcomings, the design and exploration of artificial enzyme mimics have aroused intensive interest in the field of bioassays. Recently, a series of nanomaterials defined as nanozymes such as peroxidase, catalase, superoxide dismutase, oxidase and so forth have been reported to possess unexpected and inherent enzyme-like catalytic abilities [5,6]. Despite the low price, high stability and easy preparation, nanozymes still suffer from some shortages such as low reproducibility, less specificity toward substrate, and plausible catalytic mechanism.

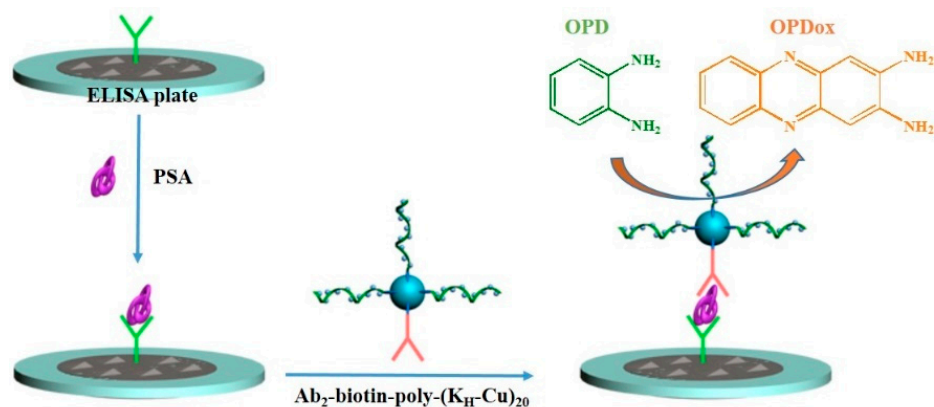
As a 3d transition metal, copper ion can accelerate a variety of reactions through a one- or two-electron pathway because of its wide range of accessible oxidation state (Cu⁰, Cu^I, Cu^{II}, and Cu^{III}) [7,8]. Copper ion plays a critical role in biological systems such as metabolic

reactions and enzyme catalysis. It has been reported that copper ion is accommodated in many metalloproteins (e.g., laccase, ceruloplasmin and ascorbate oxidase) and mainly acts as the active catalytic center to promote many redox reactions [9–11]. Mimicking the redox-active center of natural enzyme can greatly improve the catalytic ability and specificity of nanozymes based on the structure-activity relationship. Inspired by this phenomenon, many copper-functionalized metal, metal oxide and metal organic frameworks (MOFs)-based nanozymes have been synthesized through the coordination interaction and utilized to develop various biosensors. For example, Willner et al. suggested that Cu^{2+} -modified carbon nitride nanoparticles, carbon dots, graphene oxide nanoparticles and MOFs possess HRP-mimicking activity and can be used as heterogeneous catalysts to promote the generation of chemiluminescence in the presence of luminole/ H_2O_2 [12–14]. Meng et al. demonstrated that the Cu^{2+} -containing carbon dots show laccase-like activity to catalyzing the oxidation of *p*-phenylenediamine [15]. Besides, some Cu^{2+} -consisted nanomaterials show peroxidase-mimicking activity. For instance, MOF-818 with trinuclear copper centers was reported to exhibit catechol oxidase activity with excellent specificity [16]. Liu et al. found that MOFs formed by the coordination interaction between Cu^{2+} ions and guanosine monophosphates could be used as multicopper laccase mimicking nanozymes [10]. Zhao et al. suggested that copper hexacyanoferrate (Cu-HCF) nanozymes with single-site copper exhibit glutathione oxidase and peroxidase activities, which can initiate the cascade enzymatic reaction in tumor microenvironment [17]. These works suggest that copper ion can be used to design various catalysts or nanozymes with shape/size heterogeneity and high catalytic ability.

For a great majority of copper ion-containing proteins, histidine (His) residue located in different positions of peptide sequence has an important effect on the coordination of copper ion [18]. For example, peptides with a His residue in the first, second, or third position of N-terminal show different affinity capability and coordination mode towards copper ion [19–24]. We have reported that the peptide with a histidine (His) residue in the third position of N-terminal (denoted as ATCUN peptide) can limit the peroxidase and oxidase-like catalytic ability of copper ion, but the ATCUN peptide-copper complexes exhibit excellent activity for electrocatalytic water oxidation [25–27]. In this paper, we investigated the redox activity of copper ion coordinated by the peptide with a His residue in the first or second position from the N-terminus such as His-Ala (HA) and Ala-His (AH) (Scheme 1). It was found that the HA- Cu^{2+} complexes could accelerate the electrochemical reduction of O_2 and catalyze the chemical oxidation of ascorbic acid (AA) and *o*-phenylenediamine (OPD) by O_2 , but the AH peptide suppressed the electrochemical and catalytic activity of Cu^{2+} . For this fact, His was modified on the side chain amino group of biotinylated polymeric lysine (denoted as K_H) to obtain a biotin-poly- $(\text{K}_\text{H})_{20}$ polymer. The polymer can be employed as a ligand to coordinate twenty copper ions for the formation of biotin-poly- $(\text{K}_\text{H}\text{-Cu})_{20}$. The designed metal polymer was used as an artificial enzyme with multiple catalytic sites for the construction of biosensors. To demonstrate the analytical performances, prostate specific antigen (PSA), one of the most accurate and most extensively studied indicators of prostate cancer [28], was determined with the metal polymer as the signal label (Scheme 2). Biotinylated secondary antibody (Ab_2) was conjugated with the biotin-poly- $(\text{K}_\text{H}\text{-Cu}^{2+})_{20}$ polymer by using tetrameric streptavidin protein as the linker. The biotin-poly- $(\text{K}_\text{H}\text{-Cu}^{2+})_{20}$ polymer can catalyze the oxidation of OPD by O_2 to produce fluorescent 2,3-diaminophenazine (OPDox) for signal readout.



Scheme 1. Chemical structures of different Cu^{2+} complexes.



Scheme 2. Schematic illustration of fluorescent immunoassay of PSA by the biotin-poly- $(\text{K}_\text{H}\text{-Cu})_{20}$ polymer-catalyzed oxidation of OPD.

2. Experimental

2.1. Chemicals and Reagents

Peptides were obtained from ChinaPeptides. Co., Ltd. (Shanghai, China). PSA and biotinylated secondary antibody (bio- Ab_2) were provided by Linc-Bio Science Co. Ltd. (Shanghai, China). Immunoglobulin G (IgG), alpha-fetoprotein (AFP), human serum albumin (HSA) and enzyme-linked immunosorbent assay (ELISA) kits for PSA were purchased from Sigma-Aldrich. Thrombin was provided by Shanghai Yuanye Bio-Technology Co., Ltd. (Shanghai, China). Tris(hydroxymethyl)aminomethane (Tris) hydrochloride and OPD were obtained from Aladdin Corporation (Shanghai, China). Streptavidin and ascorbic acid (AA) were provided by Sangon biotech. Co., Ltd. (Shanghai, China). Human serum samples were obtained from the medical center of Anyang Normal University.

2.2. Voltammetric Characterization of Peptide- Cu^{2+}

The redox behaviors of peptide- Cu^{2+} complexes in 50 mM pH 7.0 Tris buffer were characterized by cyclic voltammetry on a CHI 660E electrochemical workstation (CH instrument, Shanghai, China). Glass carbon electrode, platinum wire and Ag/AgCl electrode were used as the working, auxiliary and reference electrodes, respectively.

2.3. Absorption Measurement of AA

AA was diluted by Tris buffer containing a given concentration of Cu^{2+} or its complexes. The peptide concentration is slightly higher than that of Cu^{2+} , ensuring that the

free Cu^{2+} is negligible. The time-resolved UV-vis absorption was recorded with a fixed wavelength of 265 nm.

2.4. Absorption Measurement of AA

To evaluate the ability of free Cu^{2+} and peptide- Cu^{2+} complexes on the oxidation of OPD, a Cu^{2+} -containing solution was mixed with the freshly prepared OPD solution at room temperature for 2 h. The mixture was then measured on a fluorescence spectrometer (Hitachi F-4600, Hitachi High-Tech, Japan).

2.5. PSA Detection

The Ab_2 -biotin-poly- $(\text{K}_\text{H}\text{-Cu})_{20}$ conjugate was prepared by mixing streptavidin with equivalent bio- Ab_2 at the concentration of 0.5 μM , followed by the addition of 1 μM biotin-poly- $(\text{K}_\text{H})_{20}$. The fluorescent immunoassays of PSA were performed in a commercialized 96-well plate. A 100 μL PSA sample at a desired concentration was added to the plate well for 30-min incubation. After that, the well was washed with phosphate buffer, followed by the addition of 100 μL of Ab_2 -biotin-poly- $(\text{K}_\text{H}\text{-Cu})_{20}$. After the formation of sandwich immunocomplex, the well was rinsed thoroughly with water and then 100 μL of Tris buffer containing 1 mM OPD was added to the well. After incubation for 1 h, the fluorescent signal was collected on the fluorescence spectrometer.

For the real sample assays, the serum samples were diluted ten times and the other procedures were the same as those for the standard sample detection. The concentrations were determined by three replicate measurements and deduced by the standard curve method.

3. Results and Discussion

3.1. Redox Behaviors of Cu^{2+} Complexes

The catalytic ability of copper complexes is greatly dependent upon the ligand nature and coordination mode. His residues in peptide play an important role in coordination of copper ions. The peptide with a His residue in the first three N-terminal positions (His^1 , His^2 and His^3) shows unique Cu^{2+} -binding property. Our group has investigated the redox property of Cu^{2+} coordinated by the ATCUN peptides with a His^3 motif in the N-terminal position [25–27]. Such ATCUN- Cu^{2+} complexes exhibit the ability for electrocatalytic water oxidation with a potential at around 0.8 V. Herein, we investigated the redox activity of Cu^{2+} coordinated by the peptide with a His residue in the first or second position from the N-terminus. As shown in Figure 1A, the cyclic voltammogram (CV) of free Cu^{2+} exhibits a redox wave with a midpoint potential ($E_{1/2}$) at around 0.05 V, which is attributed to the redox reaction of $\text{Cu}^{2+}/\text{Cu}^+$. The sharp anodic peak at -0.05 V is originated from the stripping of Cu^0 [29]. The high background at the potential below -0.3 V can be attributed to the electrochemical reduction of O_2 in solution [29]. For the HA- Cu^{2+} complex, an irreversible redox peak was observed in air-saturated solution. The redox peak became reversible when the solution was saturated by N_2 (Figure 1B). The midpoint potential (-0.012 V) is more negative than that of free Cu^{2+} . The results indicate that the electrogenerated HA- Cu^+ can be rapidly oxidized into HA- Cu^{2+} by O_2 in solution. No redox waves were observed for AH- Cu^{2+} , indicating that the complex is redox inactive in the potential between 1.0 V and -0.4 V. A similar result was obtained for KH- Cu^{2+} (Figure 1C). However, when the His residue was modified on the side chain amino group of lysine, a couple of redox waves similar to that of HA- Cu^{2+} were observed. The redox waves become more irreversible at a lower scan rate (the inset in panel C), demonstrating that the generated $\text{K}_\text{H}\text{-Cu}^+$ can be immediately oxidized into $\text{K}_\text{H}\text{-Cu}^{2+}$ by oxygen. Similar CVs were observed for the Cu^{2+} complex formed with the biotin-poly- $(\text{K}_\text{H})_{20}$ polymer (Figure 1D). The results suggest that Cu^{2+} coordinated by the peptide with a His residue in the first N-terminal position can facilitate the catalytic reduction of O_2 .

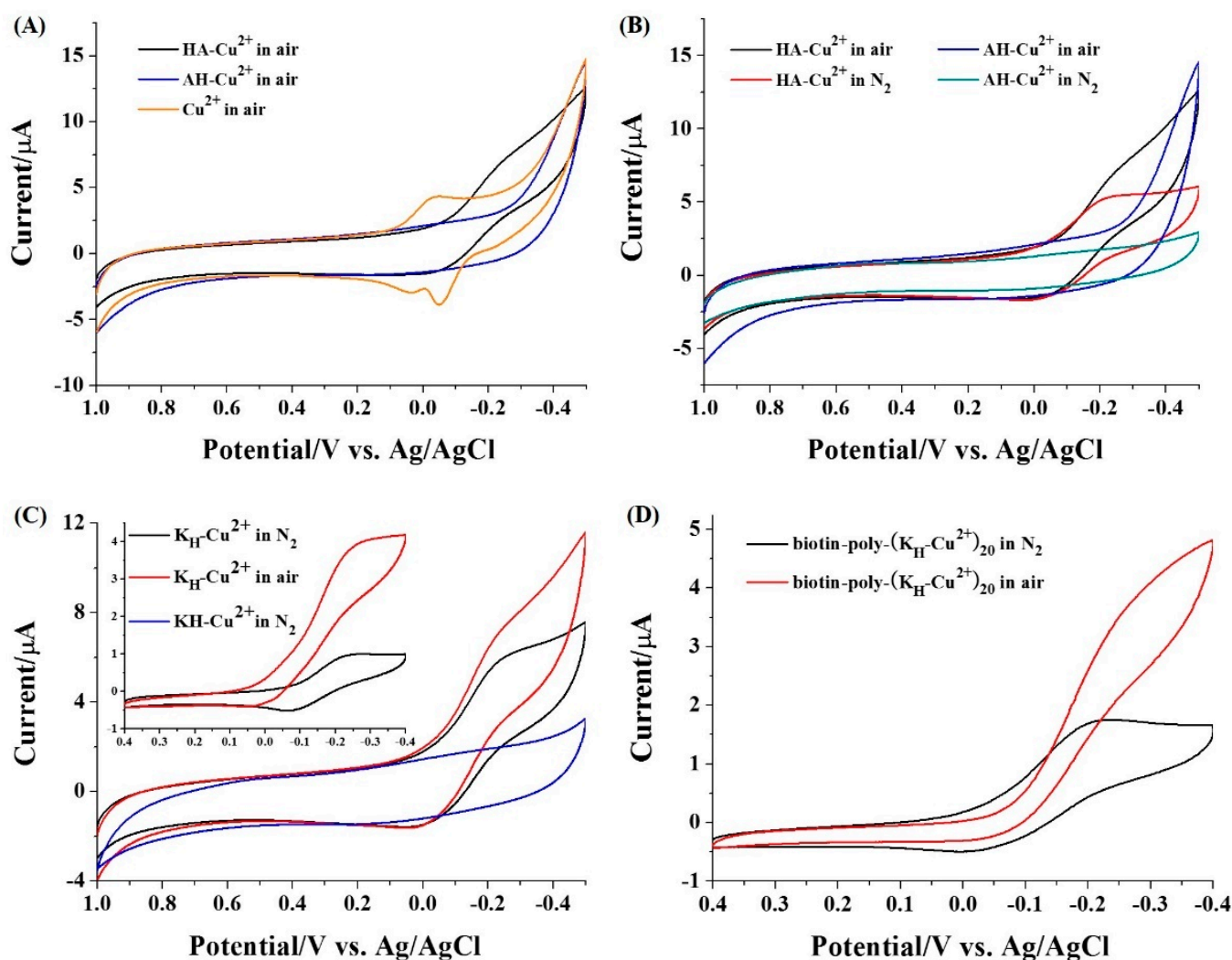


Figure 1. CVs of Cu^{2+} in air or nitrogen-saturated solution in the presence of different peptides. The scan rate was 100 mV/s (A–C) or 20 mV/s (D and the inset in figure C). The final concentrations of peptide and Cu^{2+} were 100 μM .

3.2. Catalytic Activity of Cu^{2+} Complexes

The redox potential of HA-Cu^{2+} and $\text{K}_\text{H}\text{-Cu}^{2+}$ complexes is higher than that of AA (-0.145 V) but lower than that of O_2 [29]. From the thermodynamic viewpoint, the Cu^{2+} complex can be reduced by AA and the resulting Cu^+ complex can be oxidized by O_2 , thus initiating the redox cycling between AA and O_2 . This process can be monitored by the absorbance change at 265 nm. As shown in Figure 2A, no significant change in the absorption intensity was observed for AA alone (curve 1), indicating that AA is stable at neutral pH. In the presence of a catalytic amount of free Cu^{2+} (curve 2), HA-Cu^{2+} (curve 3), $\text{K}_\text{H}\text{-Cu}^{2+}$ (curve 4), and biotin-poly- $(\text{K}_\text{H}\text{-Cu}^{2+})_{20}$ (curve 5), the absorption intensity decreased remarkably with time, indicating that these Cu^{2+} species can catalyze the oxidation of AA. The addition of AH-Cu^{2+} (curve 6) or KH-Cu^{2+} (curve 7) to the AA solution did not cause a significant decrease in the absorption intensity. Cu^{2+} can catalyze the oxidation of OPD to produce a yellow fluorescent product OPDox. Coordination of Cu^{2+} by some ligands such as quinolone, pyrophosphate, glyphosate, bleomycin, penicillamine and EDTA can inhibit the reaction between Cu^{2+} and OPD [30–35]. For this consideration, we investigated the reaction between the peptide- Cu^{2+} complexes and OPD. It was found that the peptides with a His residue in the second N-terminal position (AH and KH) depress the catalytic activity of Cu^{2+} . Interestingly, the peptides with a His residue in the first N-terminal position such as HA, K_H and biotin-poly- $(\text{K}_\text{H})_{20}$ promote the catalytic activity

of Cu^{2+} . These results indicate the Cu^{2+} complexes coordinated by the peptides with a His residue in the first N-terminal position exhibit oxidase-like activity for the oxidation of AA and OPD.

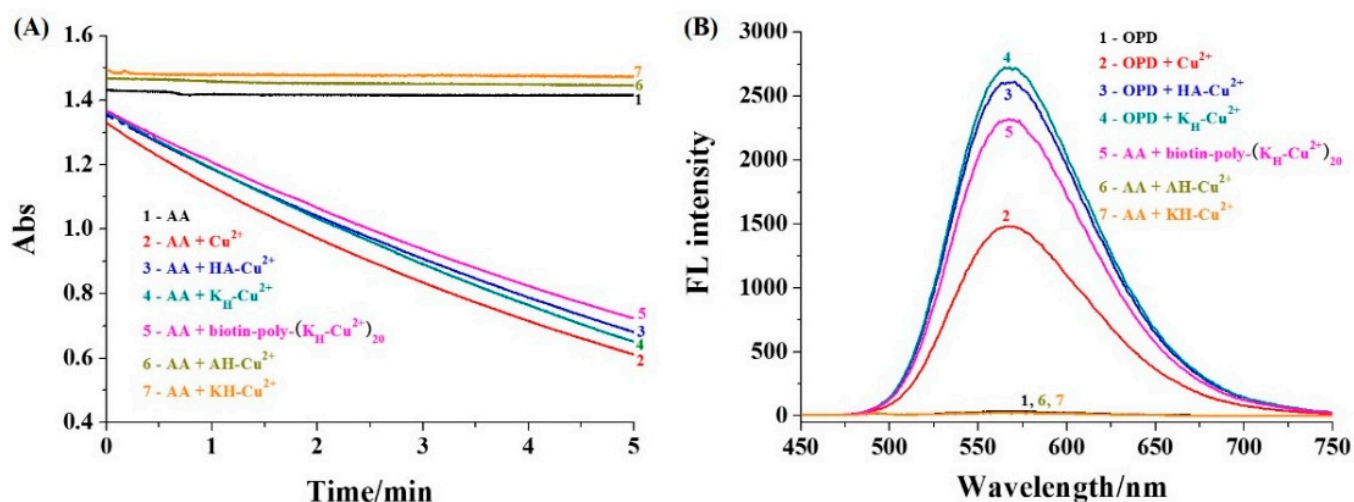


Figure 2. (A) Time-dependence of AA absorbance and (B) fluorescence spectra of OPD in the absence and presence of different Cu^{2+} -containing species. The concentrations of AA, OPD, Cu^{2+} , peptides, and biotin-poly-(K_H)₂₀ polymer were 100 μM , 2 μM , 2.5 μM and 0.1 μM , respectively.

3.3. Sensitivity of Immunoassays

The detection of protein biomarkers is of great importance for early diagnosis and treatment of many diseases. Sandwich ELISA is the most commonly used method for protein detection in clinics. PSA is a well-known biomarker for prostate patients. To demonstrate the sensitivity of our strategy, PSA was determined by using biotin-poly-(K_H - Cu^{2+})₂₀ polymer as the label for signal amplification. As shown in Scheme 2, the anti-PSA monoclonal antibody coated on the ELISA plate was used to capture PSA. The Ab₂-biotin-poly-(K_H - Cu^{2+})₂₀ conjugate formed with biotinylated anti-PSA, SA and biotin-poly-(K_H - Cu^{2+})₂₀ polymer was employed for the signal readout. As shown in Figure 3A, the fluorescence intensity was gradually intensified with the increase of PSA concentration, indicating that a higher PSA concentration could lead to the capture of more PSA molecules and signal labels on the plate. Figure 3B depicts the relationship between the fluorescence intensity and PSA concentration. The relative standard deviations (RSDs) deduced from three replicate measurements for each concentration are all lower than 9%, which is indicative of acceptable repeatability and accuracy of this method. A linear fitting curve was obtained in the concentration of 0.01 and 2 ng/mL. The linear equation can be expressed as $F = 245[\text{PSA}] (\text{ng/mL}) + 86$. The detection limit was attained as low as 8 pg/mL, which is lower than that achieved by the ELISA kit with the enzyme-catalyzed signal amplification. Moreover, the sensitivity is comparable to those of the fluorescent immunoassays by the signal amplification of nanoenzymes or enzyme-loaded nanomaterials (Table 1). The high sensitivity can be attributed to the low background signal of the sandwich-like assay and the excellent catalytic ability of the Cu^{2+} polymer for OPD oxidation. The biotin-poly-(K_H - Cu)₂₀ polymer can be readily modified on the surface of nanomaterials through the avidin-biotin interaction. We believe that the sensitivity could be further improved by increasing the length of the polymer or by using nanomaterials to load large numbers of polymers.

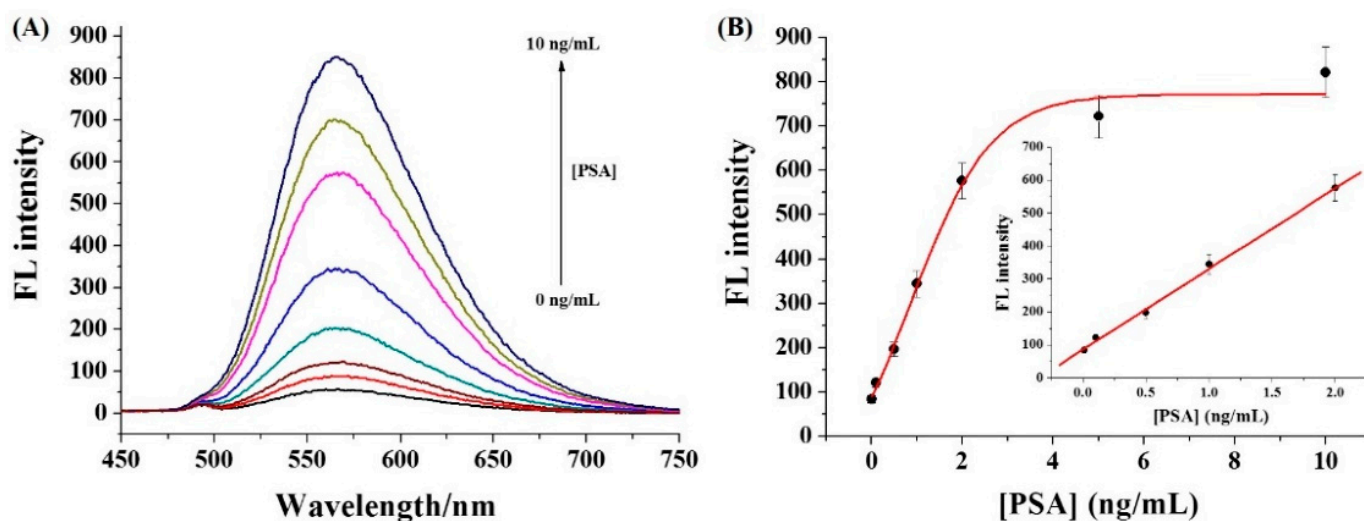


Figure 3. Fluorescence spectra (A) and plot of fluorescence intensity (B) against different PSA concentration. The inset shows the linear portion of the fitting curve.

Table 1. Analytical performances of different strategies for fluorescent immunoassays of PSA.

Supporter	Signal Reporter	Linear Range (ng/mL)	Detection Limit (ng/mL)	Refs.
Microplate	Fe-MOFs/ALP/TMB	1~20	0.18	[36]
Microplate	CsPbBr ₃ NCs/TMB	1×10^{-2} ~80	8.1×10^{-2}	[37]
Microplate	ALP/F@CNPs	0.1~50	4×10^{-2}	[38]
Microplate	ALP/Si CNPs	2×10^{-2} ~28	9.6×10^{-3}	[39]
Microplate	ZnS NCs	1×10^{-5} ~ 1×10^3	5×10^{-6}	[40]
Microplate	CuS/OPD	5×10^{-4} ~50	1×10^{-4}	[41]
Magnetic bead	CdTe@SiO ₂	1×10^{-2} ~5	3×10^{-3}	[42]
Magnetic bead	QDs	1×10^{-2} ~40	2.5×10^{-5}	[43]
Magnetic bead	GQDs@Ag	1×10^{-3} ~20	3×10^{-4}	[44]
Microplate	biotin-poly-(K _H -Cu) ₂₀	1×10^{-2} ~2	8×10^{-3}	This work

Abbreviations: Fe(III)-containing metal-organic frameworks, Fe-MOFs; alkaline phosphatase, ALP; nanocrystals, NCs; coordination nanoparticles loaded with fluorescein (F@CNPs); silicon-containing nanoparticles, Si CNPs; CuS nanoparticles, CuS NPs; graphene oxide quantum dots@silver, GQDs@Ag.

3.4. Selectivity and Real Sample Assays

Selectivity is the basic requirement for the practical reliability of biosensors. The biosensor was challenged by determining low concentration of PSA and high concentration of interfering proteins. As depicted in Figure 4, no significant signals were observed for the tested interfering proteins, which is indicative of the excellent selectivity of the method. This can be attributed to the specific antigen-antibody interaction and the low non-specific adsorption of the polymer label. Female serum contains a negligible content of PSA. To demonstrate the anti-interference, female serum was spiked with PSA for assay. The result obtained in the female serum was consistent with that found in the buffer, indicating that the detection in the serum was interference-free. Encouraged by the result, PSA in three male serum samples was determined by this method and the commercialized ELISA kit (Table 2). The samples were diluted 10 times to ensure that the PSA concentration was in the linear range of the standard curve. The results obtained by our method are well coincident with those achieved by the commercial ELISA kit, demonstrating that the polymer label can be used to replace the enzyme label in clinical diagnosis. In contrast to the enzyme label, the polymer label shows the advantages of low manufacturing cost and ease of adjustability. Moreover, the RSDs deduced from three replicate measurements by this method are lower than those obtained by the ELISA, and no decrease in the signal was

observed when the biotin-poly-(KH)₂₀ polymer was kept at room temperature for at least five months, indicating the high thermodynamic stability of the polymer label.

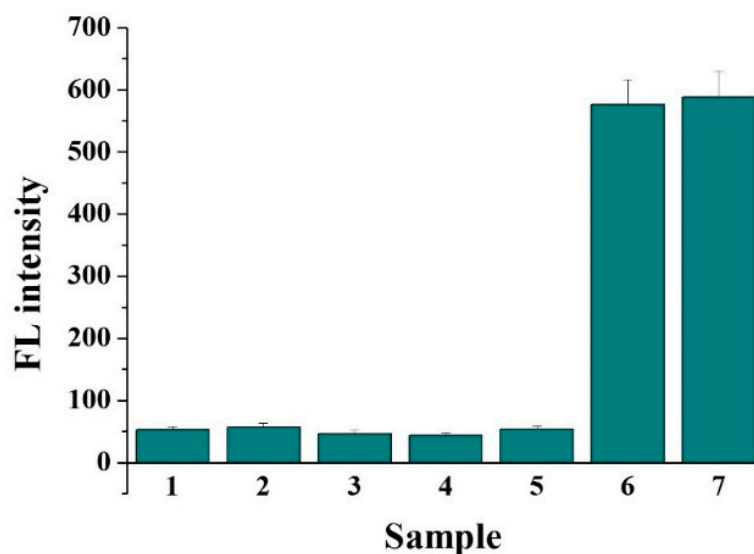


Figure 4. Selectivity of the method toward different samples: buffer blank (bar 1), 0.5 µg/mL IgG (bar 2), 0.1 µg/mL HSA (bar 3), 10 ng/mL thrombin (bar 4), 50 ng/mL AFP (bar 5) and 2 ng/mL PSA in the buffer (bar 6) or the diluted female serum (bar 7).

Table 2. Results for the assays of PSA in serum samples.

Sample No.	Found (ng/mL)	ELISA (ng/mL)
1	0.182 ± 0.012	0.171 ± 0.018
2	0.087 ± 0.007	0.094 ± 0.011
3	0.154 ± 0.013	0.132 ± 0.015

4. Conclusions

In summary, we have investigated the electrochemical and catalytic activities of different peptide-Cu²⁺ complexes and designed a metal polymer for the development of immunoassays. The resulting biotin-poly-(KH)₂₀ polymer was successfully used as an artificial enzyme label for PSA detection. Benefiting from the excellent analytical performances, the immunoassays achieved a low detection limit. The method was successfully used to detect PSA in real serum samples. The results are in agreement with those achieved by the commercial ELISA kit, indicating the great potential applications of the method for clinical assays of different biomarkers. Moreover, the polymer label exhibits the advantages of low cost and high stability and could be readily modified on the surface of nanomaterials to improve the sensitivity of immunoassays. We believe that this strategy can pave a new way to develop different sensing platforms for biomarker detection.

Author Contributions: Conceptualization, Y.F. and L.L.; methodology, Y.F. and Y.L.; investigation, Y.F., G.L., C.Z. and J.L.; writing—original draft preparation, Y.F.; writing—review and editing, Y.L.; project administration, L.L.; funding acquisition, L.L. All authors have read and agreed to the published version of the manuscript.

Funding: This research was funded by the Program for Innovative Research Team of Science and Technology in the University of Henan Province (21IRTSTHN005) and the National Natural Science Foundation of China (U2004193).

Institutional Review Board Statement: Not applicable.

Informed Consent Statement: Not applicable.

Data Availability Statement: Not applicable.

Conflicts of Interest: The authors declare no conflict of interest.

Sample Availability: Not applicable.

References

1. Radha, R.; Shahzadi, S.K.; Al-Sayah, M.H. Fluorescent immunoassays for detection and quantification of cardiac troponin I: A short review. *Molecules* **2021**, *26*, 4812. [[CrossRef](#)] [[PubMed](#)]
2. Wang, Y.; Xianyu, Y. Nanobody and nanozyme-enabled immunoassays with enhanced specificity and sensitivity. *Small Methods* **2022**, *6*, 2101576. [[CrossRef](#)]
3. Zhao, Q.; Lu, D.; Zhang, G.; Zhang, D.; Shi, X. Recent improvements in enzyme-linked immunosorbent assays based on nanomaterials. *Talanta* **2021**, *223*, 121722. [[CrossRef](#)]
4. Gao, L.; Yang, Q.; Wu, P.; Li, F. Recent advances in nanomaterial-enhanced enzyme-linked immunosorbent assays. *Analyst* **2020**, *145*, 4069–4078. [[CrossRef](#)]
5. Liang, M.; Yan, X. Nanozymes: From new concepts, mechanisms, and standards to applications. *Acc. Chem. Res.* **2019**, *52*, 2190–2200. [[CrossRef](#)] [[PubMed](#)]
6. Wu, J.; Wang, X.; Wang, Q.; Lou, Z.; Li, S.; Zhu, Y.; Qin, L.; Wei, H. Nanomaterials with enzyme-like characteristics (nanozymes): Next-generation artificial enzymes (II). *Chem. Soc. Rev.* **2019**, *48*, 1004–1076. [[CrossRef](#)]
7. Tian, S.; Zeng, K.; Yang, A.; Wang, Q.; Yang, M. A copper based enzyme-free fluorescence ELISA for HER2 detection. *J. Immunol. Methods* **2017**, *451*, 78–82. [[CrossRef](#)]
8. Drommi, M.; Rulmont, C.; Esmieu, C.; Hureau, C. Hybrid bis-histidine phenanthroline-based ligands to lessen A β -bound Cu ROS production: An illustration of Cu(I) significance. *Molecules* **2021**, *26*, 7630. [[CrossRef](#)] [[PubMed](#)]
9. Mitra, S.; Prakash, D.; Rajabimoghadam, K.; Wawrzak, Z.; Prasad, P.; Wu, T.; Misra, S.K.; Sharp, J.S.; Garcia-Bosch, I.; Chakraborty, S. De novo design of a self-assembled artificial copper peptide that activates and reduces peroxide. *ACS Catal.* **2021**, *11*, 10267–10278. [[CrossRef](#)]
10. Liang, H.; Lin, F.; Zhang, Z.; Liu, B.; Jiang, S.; Yuan, Q.; Liu, J. Multicopper laccase mimicking nanozymes with nucleotides as ligands. *ACS Appl. Mater. Interfaces* **2017**, *9*, 1352–1360. [[CrossRef](#)]
11. Zhang, X.; Wu, D.; Wu, Y.; Li, G. Bioinspired nanozyme for portable immunoassay of allergenic proteins based on A smartphone. *Biosens. Bioelectron.* **2021**, *172*, 112776. [[CrossRef](#)]
12. Chen, W.-H.; Vázquez-González, M.; Kozell, A.; Ceconello, A.; Willner, I. Cu²⁺-modified metal–organic framework nanoparticles: A peroxidase-mimicking nanoenzyme. *Small* **2018**, *14*, 1703149. [[CrossRef](#)] [[PubMed](#)]
13. Vázquez-González, M.; Liao, W.-C.; Cazelles, R.; Wang, S.; Yu, X.; Gutkin, V.; Willner, I. Mimicking horseradish peroxidase functions using Cu²⁺-modified carbon nitride nanoparticles or Cu²⁺-modified carbon dots as heterogeneous catalysts. *ACS Nano* **2017**, *11*, 3247–3253. [[CrossRef](#)]
14. Wang, S.; Cazelles, R.; Liao, W.-C.; Vázquez-González, M.; Zoabi, A.; Abu-Reziq, R.; Willner, I. Mimicking horseradish peroxidase and NADH peroxidase by heterogeneous Cu²⁺-modified graphene oxide nanoparticles. *Nano Lett.* **2017**, *17*, 2043–2048. [[CrossRef](#)]
15. Ren, X.; Liu, J.; Ren, J.; Tang, F.; Meng, X. One-pot synthesis of active copper-containing carbon dots with laccase-like activities. *Nanoscale* **2015**, *7*, 19641–19646. [[CrossRef](#)] [[PubMed](#)]
16. Li, M.; Chen, J.; Wu, W.; Fang, Y.; Dong, S. Oxidase-like MOF-818 nanozyme with high specificity for catalysis of catechol oxidation. *J. Am. Chem. Soc.* **2020**, *142*, 15569–15574. [[CrossRef](#)]
17. Wang, D.; Wu, H.; Wang, C.; Gu, L.; Chen, H.; Jana, D.; Feng, L.; Liu, J.; Wang, X.; Xu, P.; et al. Self-assembled single-site nanozyme for tumor-specific amplified cascade enzymatic therapy. *Angew. Chem. Int. Ed.* **2021**, *60*, 3001–3007. [[CrossRef](#)] [[PubMed](#)]
18. Sóvágó, I.; Várnagy, K.; Lihí, N.; Grenács, Á. Coordinating properties of peptides containing histidyl residues. *Coord. Chem. Rev.* **2016**, *327–328*, 43–54. [[CrossRef](#)]
19. May, N.V.; Jancsó, A.; Enyedy, É.A. Binding models of copper(II) thiosemicarbazone complexes with human serum albumin: A speciation study. *Molecules* **2021**, *26*, 2711. [[CrossRef](#)]
20. Portelinha, J.; Duay, S.S.; Yu, S.I.; Heilemann, K.; Libardo, M.D.J.; Juliano, S.A.; Klassen, J.L.; Angeles-Boza, A.M. Antimicrobial peptides and copper(II) ions: Novel therapeutic opportunities. *Chem. Rev.* **2021**, *121*, 2648. [[CrossRef](#)] [[PubMed](#)]
21. Fraczyk, T. Cu(II)-binding N-terminal sequences of human proteins. *Chem. Biodivers.* **2021**, *18*, e2100043. [[CrossRef](#)]
22. Mena, S.; Mirats, A.; Caballero, A.B.; Guirado, G.; Barrios, L.A.; Teat, S.J.; Rodriguez-Santiago, L.; Sodupe, M.; Gamez, P. Drastic effect of the peptide sequence on the copper-binding properties of tripeptides and the electrochemical behaviour of their copper(II) complexes. *Chem. Eur. J.* **2018**, *24*, 5153–5162. [[CrossRef](#)] [[PubMed](#)]
23. Harford, C.; Sarkar, B. Amino terminal Cu(II)- and Ni(II)-binding (ATCUN) motif of proteins and peptides: Metal binding, DNA cleavage, and other properties. *Acc. Chem. Res.* **1997**, *30*, 123–130. [[CrossRef](#)]
24. Gonzalez, P.; Bossak, K.; Stefaniak, E.; Hureau, C.; Raibaut, L.; Bal, W.; Faller, P. N-Terminal Cu-binding motifs (Xxx-Zzz-His, Xxx-His) and their derivatives: Chemistry, biology and medicinal applications. *Chem. Eur. J.* **2018**, *24*, 8029–8041. [[CrossRef](#)] [[PubMed](#)]

25. Xia, N.; Deng, D.; Yang, S.; Hao, Y.; Wang, L.; Liu, Y.; An, C.; Han, Q.; Liu, L. Electrochemical immunosensors with protease as the signal label for the generation of peptide-Cu(II) complexes as the electrocatalysts toward water oxidation. *Sens. Actuators B Chem.* **2019**, *291*, 113–119. [[CrossRef](#)]
26. Liu, L.; Deng, D.; Wang, Y.; Song, K.; Shang, Z.; Wang, Q.; Xia, N.; Zhang, B. A colorimetric strategy for assay of protease activity based on gold nanoparticle growth controlled by ascorbic acid and Cu(II)-coordinated peptide. *Sens. Actuators B Chem.* **2018**, *266*, 246–254. [[CrossRef](#)]
27. Deng, D.; Liu, L.; Bu, Y.; Liu, X.; Wang, X.; Zhang, B. Electrochemical sensing devices using ATCUN-Cu(II) complexes as electrocatalysts for water oxidation. *Sens. Actuators B Chem.* **2018**, *269*, 189–194. [[CrossRef](#)]
28. Özyurt, C.; Uludağ, İ.; İnce, B.; Sezgintürk, M.K. Biosensing strategies for diagnosis of prostate specific antigen. *J. Pharmaceut. Biomed. Anal.* **2022**, *209*, 114535. [[CrossRef](#)] [[PubMed](#)]
29. Liu, L.; Jiang, D.; McDonald, A.; Hao, Y.; Millhauser, G.L.; Zhou, F. Copper redox cycling in the prion protein depends critically on binding mode. *J. Am. Chem. Soc.* **2011**, *133*, 12229–12237. [[CrossRef](#)]
30. Yang, D.; Li, Q.; Tammina, S.K.; Gao, Z.; Yang, Y. Cu-CDs/H₂O₂ system with peroxidase-like activities at neutral pH for the co-catalytic oxidation of o-phenylenediamine and inhibition of catalytic activity by Cr(III). *Sens. Actuators B Chem.* **2020**, *319*, 128273. [[CrossRef](#)]
31. Sun, J.; Wang, B.; Zhao, X.; Li, Z.-J.; Yang, X. Fluorescent and colorimetric dual-readout assay for inorganic pyrophosphatase with Cu²⁺-triggered oxidation of ophenylenediamine. *Anal. Chem.* **2016**, *88*, 1355–1361. [[CrossRef](#)]
32. Yang, X.; Wang, E. A nanoparticle autocatalytic sensor for Ag⁺ and Cu²⁺ ions in aqueous solution with high sensitivity and selectivity and its application in test paper. *Anal. Chem.* **2011**, *83*, 5005–5011. [[CrossRef](#)] [[PubMed](#)]
33. Zhu, S.; Cao, H.; Yan, X.; Sun, J.; Qiu, J.; Qu, X.; Zuo, Y.-N.; Wang, X.; Zhao, X.-E. A convenient fluorescent assay for quinolones based on their inhibition towards the oxidase-like activity of Cu²⁺. *New J. Chem.* **2019**, *43*, 3707–3712. [[CrossRef](#)]
34. Yang, Y.; Li, L.; Lin, L.; Wang, X.; Li, J.; Liu, H.; Liu, X.; Huo, D.; Hou, C. A dualsignal sensing strategy based on ratiometric fluorescence and colorimetry for determination of Cu²⁺ and glyphosate. *Anal. Bioanal. Chem.* **2022**, *414*, 2619–2628. [[CrossRef](#)]
35. Zhang, W.; Zhang, Y.; Liu, X.; Zhang, Y.; Liu, Y.; Wang, W.; Su, R.; Sun, Y.; Huang, Y.; Song, D.; et al. Ratiometric fluorescence and colorimetric dual-mode sensing platform based on carbon dots for detecting copper(II) ions and D-penicillamine. *Anal. Bioanal. Chem.* **2022**, *414*, 1651–1662. [[CrossRef](#)] [[PubMed](#)]
36. Xie, W.; Tian, M.; Luo, X.; Jiang, Y.; He, N.; Liao, X.; Liu, Y. A dual-mode fluorescent and colorimetric immunoassay based on in situ ascorbic acid-induced signal generation from metal-organic frameworks. *Sens. Actuators B Chem.* **2020**, *302*, 127180. [[CrossRef](#)]
37. Li, M.; Wang, Y.; Hu, H.; Feng, Y.; Zhu, S.; Li, C.; Feng, N. A dual-readout sandwich immunoassay based on biocatalytic perovskite nanocrystals for detection of prostate specific antigen. *Biosens. Bioelectron.* **2022**, *203*, 113979. [[CrossRef](#)]
38. Sun, C.; Shi, Y.; Tang, M.; Hu, X.; Long, Y.; Zheng, H. A signal amplification strategy for prostate specific antigen detection via releasing oxidase-mimics from coordination nanoparticles by alkaline phosphatase. *Talanta* **2020**, *213*, 120827. [[CrossRef](#)]
39. Chen, C.; Zhao, D.; Wang, B.; Ni, P.; Jiang, Y.; Zhang, C.; Yang, F.; Lu, Y.; Sun, J. Alkaline phosphatase-triggered in situ formation of silicon-containing nanoparticles for a fluorometric and colorimetric dual-channel immunoassay. *Anal. Chem.* **2020**, *92*, 4639–4646. [[CrossRef](#)]
40. Hu, R.; Liu, T.; Zhang, X.-B.; Yang, Y.; Chen, T.; Wu, C.; Liu, Y.; Zhu, G.; Huan, S.; Fu, T.; et al. DLISA: A DNzyme-based ELISA for protein enzyme-free immunoassay of multiple analytes. *Anal. Chem.* **2015**, *87*, 7746–7753. [[CrossRef](#)] [[PubMed](#)]
41. Zhu, Y.-D.; Peng, J.; Jiang, L.-P.; Zhu, J.-J. Fluorescent immunosensor based on CuS nanoparticles for sensitive detection of cancer biomarker. *Analyst* **2014**, *139*, 649–655. [[CrossRef](#)] [[PubMed](#)]
42. Zhao, Y.; Gao, W.; Ge, X.; Li, S.; Du, D.; Yang, H. CdTe@SiO₂ signal reporters-based fluorescent immunosensor for quantitative detection of prostate specific antigen. *Anal. Chim. Acta* **2019**, *1057*, 44–50. [[CrossRef](#)] [[PubMed](#)]
43. Cao, D.; Li, C.-Y.; Qi, C.-B.; Chen, H.-L.; Pang, D.-W.; Tang, H.-W. Multiple optical trapping assisted bead-array based fluorescence assay of free and total prostate-specific antigen in serum. *Sens. Actuators B Chem.* **2018**, *269*, 143–150. [[CrossRef](#)]
44. Pei, H.; Zhu, S.; Yang, M.; Kong, R.; Zheng, Y.; Qu, F. Graphene oxide quantum dots@silver core-shell nanocrystals as turn-on fluorescent nanoprobe for ultrasensitive detection of prostate specific antigen. *Biosens. Bioelectron.* **2015**, *74*, 909–914. [[CrossRef](#)]